ChemComm

Development of a Novel Durable Aromatic Anion Exchange Membrane using a Thermally Convertible Precursor

Journal:	*ChemComm*
Manuscript ID	CC-COM-07-2018-005371.R2
Article Type:	Communication

ChemComm

COMMUNICATION

Development of a Novel Durable Aromatic Anion Exchange Membrane using a Thermally Convertible Precursor

Received 00th January 20xx,
Accepted 00th January 20xx

DOI: 10.1039/x0xx00000x

www.rsc.org/

Hafis P. R. Graha[a], Shinji Ando[b], Shoji Miyanishi[a,c], and Takeo Yamaguchi*[a,b,c]

We describe a new approach for obtaining high performance anion exchange membranes by using a thermally convertible precursor. A new insoluble all-aromatic polymer containing anthracene units and benzyl trimetyl ammonium was successfully prepared from a highly soluble precursor polymer. The resulting polymer shows excellent chemical durability and conductivity.

Membrane has been an important component in the sustainable energy production devices such as solar cells, batteries, and fuel cells. It needs not only good performance but also excellent durability[1–6]. Solid alkaline fuel cells (SAFCs) using anion exchange membranes (AEM) are a low-cost and high-efficiency alternative to the commercially and widely used proton exchange membrane fuel cells (PEMFCs)[7]. These SAFCs have recently attracted some attention in fuel cell system development owing to the tolerance of metal catalysts against corrosion in a high pH environment, a property that is expected to facilitate the use of cheaper nonprecious metal catalysts[8], low fuel crossover[9], and alternative fuels such as ammonia, methanol, ethanol, formate, and ethylene glycol[10,11].

Despite the considerable number of advantages that the use of SAFCs provides, several drawbacks of AEMs prevent their commercialization. The major challenges in AEM development include its chemical durability and ionic conductivity[12,13]. In terms of durability, it is well known that the stability of AEM in hot alkaline solution is low. Although the low stability of the anion exchange group is generally believed to be the main reason for the degradation of AEMs, a recently proposed degradation mechanism of typical polyethersulfone-based AEM suggests that the hydroxyl ion attacks the ether bond on the polymer backbone, inducing rapid deactivation of the anion exchange site[14,15]. Theoretical calculations also indicate that AEM degradation mainly occurs on the backbone in typical polyarylene ether AEMs[16,17]. To prevent backbone degradation, heteroatom-free fully aromatic polyphenylene constitutes a promising alternative.

The development of such type of polymers is also advantageous from the viewpoint of ion conductivity. A good AEM should exhibit high ionic conductivity (typically $\geq 10^{-2}$ S/cm) to minimize resistive losses[18]. However, in typical AEMs, such levels of conductivity can be only obtained by increasing the amount of ion exchange sites (higher ion exchange capacity – IEC). Under this condition, the membrane inevitably suffers from significant swelling, which leads to low mechanical stability. The introduction of strong intermolecular interactions in the polymer through crystallization or heteroatom interactions has proven to be effective for suppressing swelling of the membrane. Therefore, swelling can be expected to be effectively suppressed in fully aromatic polymers, since these planar conjugated polymers show typically very strong intermolecular π–π interactions. However, this strong intermolecular interactions drastically lower the polymer solubility in common organic solvent, which hinders preparation of the membrane film[19]. In this context, several strategies have been attempted with the aim of creating fully aromatic backbone AEMs. Recently, polyphenylene-based AEMs having bulky side group[20], using long spacer side chains[21], with a meta-phenylene structure[21], and other containing piperidinium groups in the backbone[22] have been reported. In addition, an AEM with perfluoroalkylene and fluorenyl groups in the backbone and pendant ammonium groups has been described[23].

Herein, we propose the design of a novel AEM based on a precursor polymer with temporarily disrupted π–π interactions that will exhibit all the advantages of an aromatic backbone polymer with properties that can be easily processed. In this study, we use anthracene, a simple group, as the hydrophobic section and benzyltrimethylammonium (BTMA) as the hydrophilic section of the backbone. The precursor polymer itself should have high solubility in common organic solvents in order to ensure the easy fabrication of the membrane. To

[a] Laboratory for Chemistry and Life Science, Tokyo Institute of Technology, 4259 Nagatsuta, Midori-ku, Yokohama 226-8503, Japan. E-mail: yamag@res.titech.ac.jp (T.Y.)
[b] Kanagawa Institute of Industrial Science and Technology (KISTEC), Japan.
[c] Core Research for Evolutionary Science and Technology, Japan Science and Technology Agency (JST-CREST), Japan
† Electronic Supplementary Information (EI) available. See DOI: 10.1039/x0xx00000x

provide the anthracene with thermal convertibility, a thermal leaving group (TLG) is attached through a Diels–Alder reaction. Then, the TLG can be removed via thermal annealing at a certain temperature to trigger a retro Diels–Alder reaction after the membrane film is obtained. Several studies, mainly on organic thin-film transistors, have shown that polymer solubility can be enhanced using the abovementioned approach because of the disruption of the π-stacked structure[19,24–26]. To the best of our knowledge, this is the first report on the preparation of an AEM using this approach. This method offers the possibility of obtaining highly rigid all-aromatic AEMs, which are promising materials from the viewpoint of chemical durability and swelling suppression that are difficult to prepare by conventional synthetic methods.

Scheme 1 shows the synthetic method for our target polymer. The precursor polymer bearing methyl groups (**PP1)** was synthesized via Suzuki polycondensation using monomers **2** and **4** (Scheme 1). The bromination of the methyl groups of **PP1** was performed using *N*-bromosuccinimide as a bromine source and azobisisobutyronitrile as the radical initiator. In this study, 85% of the methyl groups were brominated and subsequently quantitatively quaternized (see Supporting Information for the calculation method). BTMA was employed as anion exchange group for this polymer due to its simple preparation and good stability in harsh alkaline condition as long as the backbone is stable[14,17].

Scheme 1 Synthesis of **P-PAPP** and **PAPP.**

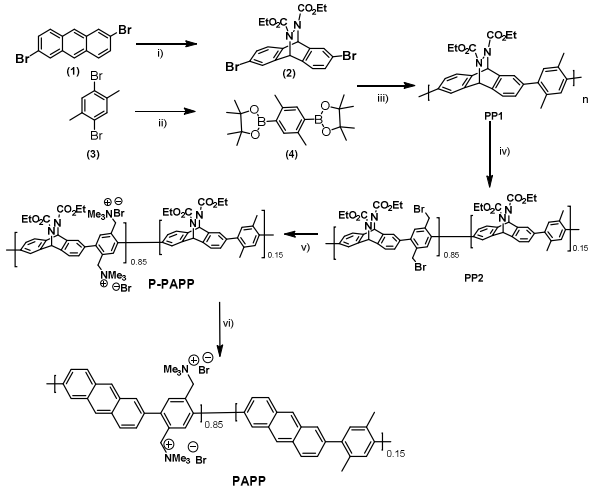

(i) Diethyl azodicarboxylate (DEAD), toluene, reflux; (ii) Bis(pinacolato)diboron, DMF, KOAc, $Pd(dppf)Cl_2$, 90 °C; (iii) toluene, $K_3PO_{4(aq)}$, $Pd(PPh_3)_4$, aliquat 336, 100 °C; (iv) NBS, AIBN, chlorobenzene, 110 °C; (v) DMF/THF, 50 °C; (vi) 180 °C.

The molecular structure of **precursor-poly(2,6-anthracene-*alt*-1,4-paraphenylene) (P-PAPP)** was characterized using ^{1}H-NMR spectroscopy (Fig. S3). The molecular weight of precursor polymer **PP2** was determined to be M_n = 1.3 x 10^4 g/mol and the polydispersion index (PDI) = 1.8 by gel permeation chromatography (GPC). It should be noted that we have estimated the molecular weight of **PP2** but not that of **P-PAPP** because of the inherent difficulty in the evalution of the molecular weight of quaternized polymers[27]. We assumed that the molecular weight of the polymer did not change significantly after quaternization.

A membrane film was successfully fabricated from **P-PAPP** by casting a membrane solution (20 wt%) in 50%–50% dimethyl formamide(DMF)–N-methylpyrolidone (NMP) onto a polytetrafluoroethylene (PTFE) substrate and letting it dry overnight at 50 °C. Thermal degradation of **P-PAPP** was evaluated by thermogravimetric–mass spectrometry (TG–MS) analysis (Fig. 1), according to which **P-PAPP** degradation was divided into two major steps. The first step started around 160 °C and involved the removal of the TLG, as indicated by the detection of an ethyl ester carboxylic fragment (Mz:73). In the second step, which started around 200 °C, the detection of the trimethylammonium fragment (Mz:59) was indicative of the degradation of the quaternary ammonium group. These data suggest that the optimal temperature for the retro Diels–Alder reaction should be around 160 °C to 200 °C to avoid degradation of the ion exchange site. In our work, the dried **P-PAPP** membrane was annealed at 180 °C for 60 min to obtain the **poly(2,6-anthracene-*alt*-1,4-paraphenylene) (PAPP**) membrane, which was accompanied by a color change from yellow (**P-PAPP**) to shiny reddish black (**PAPP**). We also tested a model low molecular compound to evaluate the stability of BTMA in the polymer at 180 °C for 60 min. The ^{1}H-NMR profile depicted in Fig. S6 shows that BTMA was very stable under the conditions of the retro Diels–Alder reaction.

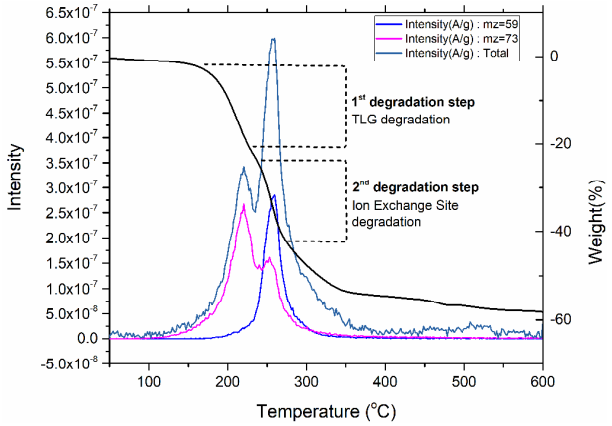

Fig. 1. TG–MS profile of **P-PAPP.**

The solubility of the **P-PAPP** membrane was greater than 300 mg/ml in DMF, and it could be dissolved even in hot water, whereas the **PAPP** membrane was almost insoluble in any solvent (Fig. S4). This indicates that the polymer backbone structure became planar and a strong intermolecular interaction appeared after thermal annealing[28], which was supported by the result of a UV–vis absorption analysis (Fig. S8). The UV spectrum of **PAPP** exhibited an intensity peak at higher wavelength than that of **P-PAPP**. From the infrared (IR) spectra, we inferred that there was a chemical change in the polymer due to the removal of the TLG upon heating (Fig. 2). A peak at 1593 cm^{-1} attributable to C=C stretching in the aromatic ring became visible after annealing, which

constituted further evidence of the removal of the TLG and the presence of the anthracene group. We estimated the TLG removal efficiency as 83% by comparing the theoretical and actual mass difference before and after the retro Diels–Alder reaction.

The theoretical IEC of **P-PAPP** was calculated to be 2.79 assuming 85% bromination, and it was expected to increase to 3.25 after annealing for the estimated TLG removal efficiency value of 83%. The IEC values experimentally determined by titration were 2.49 for **P-PAPP** and 3.16 for **PAPP**, which are in close accordance with the predicted values. Since the water uptake of **PAPP** was lower than that of **P-PAPP** in spite of the higher IEC of the former polymer (Fig. S7), it can be concluded that the swelling suppression strategy based on the π–π interactions was successful.

The conductivity evaluation was performed in HCO_3^- form to avoid the bias value from CO_2 poisoning that results from the use of the OH^- form. The **PAPP** membrane was immersed in 1 M $NaHCO_3$ solution for 48 h at room temperature to change the counterion from Br^- to HCO_3^-. The membrane was then washed thoroughly and kept at deionized (DI) water for at least 24 h before performing the conductivity measurement. From Fig.3, it can be clearly extracted that the conductivity of the **PAPP** membrane depends on relative humidity, as is observed in typical ion conductive membranes. The bicarbonate conductivity of **PAPP** was 44 mS/cm (80 °C in water), which is lower than the expected value for OH^- conductivity under the same condition[29,30].

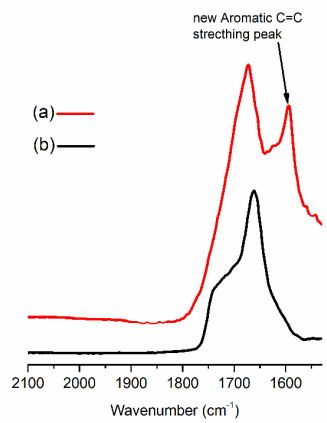

Fig. 2. ATR–IR spectra of **(a)** the **PAPP** membrane (annealed at 180 °C for 60 min) and **(b)** the **P-PAPP** membrane.

The durability of the **PAPP** membrane was evaluated by means of alkaline and oxidative durability tests. We exposed the membrane to very harsh alkaline condition, 8 M NaOH, for 21 days at 80 °C to assess its alkaline durability. Then, the membrane was put into 1M $NaHCO_3$ for 24 h, followed by immersion into DI water for further 24 h to remove the excess ions. Meanwhile, its oxidative stability was evaluated by soaking the **PAPP** membrane in Fenton solution, consisting of 3 wt% H_2O_2 and 3 ppm $FeSO_4$, at 60 °C for 8 h. The sample was then washed and kept in DI water for 24 h. The conductivity was measured in DI water. Fig. 4 and Fig. 5 show the HCO_3^- conductivity before and after the durability test. As

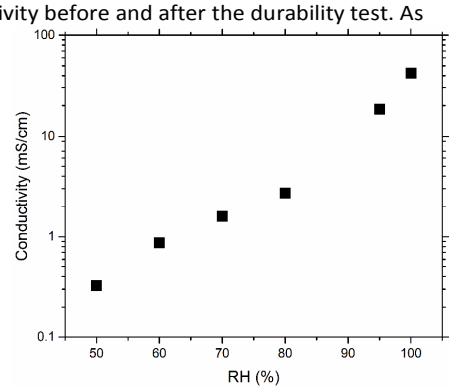

Fig. 3. PAPP membrane HCO_3^- conductivity in various RH at 80 °C.

can be seen, the conductivity remained virtually unaltered after the exposure to very harsh alkaline condition at high temperature. The same tendency was observed in the oxidative stability test, indicating that the membrane has an excellent durability in harsh alkaline and oxidative environment. In addition, **PAPP** retained 97% of its initial mass after the oxidative stability test.

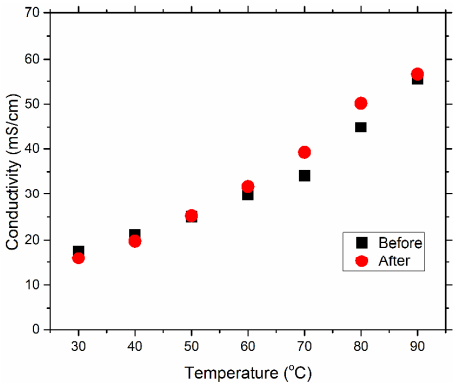

Fig. 4. Profile of **PAPP** membrane HCO_3^- conductivity before and after alkaline durability test.

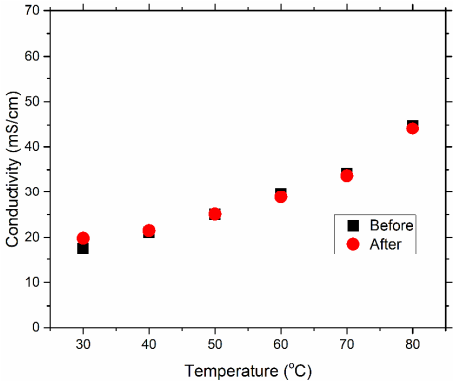

Fig. 5. Profile of **PAPP** membrane HCO_3^- conductivity before and after oxidative durability test.

Table 1 summarizes the performance of the **PAPP** membrane**,** along with that of other reported AEMs with different backbone structure for comparison. **PAPP** outperforms the linear and heteroaromatic-based AEMs that contain ether, ether–sulfone, and ether–ketone linkages.

In summary, we developed an AEM using a novel design concept involving a TLG. The developed AEM shows high chemical durability owing to a heteroatom-free backbone and high ion conductivity with minimum swelling, despite having a very high IEC. Although the preparation of this polymer is difficult by conventional synthetic methods due to its insolubility, it was readily fabricated through thermal annealing of a highly soluble precursor polymer. We believe that this new concept will facilitate the production of high performance membranes for SAFCs.

This study was supported by the Kanagawa Academy of Science and Technology, Core Research for Evolutionary Science and Technology (JPMJCR1543) at the Japan Science and Technology Agency, and KAKENHI (26820355 for S.A.).

Conflicts of interest

There are no conflicts to declare.

Table 1. Comparison of conductivity and durability performance of several AEMs

AEM	Backbone type	Ion exchange site type	IEC (g/mol)	σ (mS/cm) (OH^-)	σ (mS/cm) ($HCO3^-$)	Oxidative durability (remain mass)	Alkaline durability (remain conductivity)	Reference
PAPP	Fully aromatic	BTMA	3.16	n.a.	17 (30 °C)	97% (8h at 60 °C in fenton solution)	Almost no change (8 M NaOH at 80 °C for 500 h)	This work
BTMA40	Aromatic with ether linkage	BTMA	2.59	24 (30 °C)	n.a.	n.a	40% (1 M NaOH at 80 °C for 500 h)	[31]
Pore filling - (PVBTAC)	Aliphatic	BTMA	2.26	37 (30 °C)	n.a.	36% (8h at 60 °C in fenton solution)	Almost no change (1 M KOH at 60 °C for 720 h)	[32]
TMBA-60-3	Aromatic with ether–sulfone linkage	BTMA	1.9	n.a.	11 (30 °C)	n.a.	45% (1 M NaOH at 90 °C for 500 h)	[33]
AD30i-OH	Aromatic with ether–ketone linkage	BTMA	1	12[a] (20 °C)	n.a.	94% (12h at 60 °C in fenton solution)	50% (2 M NaOH at 60 °C for 24 h)	[34]

References

1 N. N. M. Radzir, S. A. Hanifah, A. Ahmad, N. H. Hassan and F. Bella, *J. Solid State Electrochem.*, 2015, **19**, 3079–3085.
2 L. Chen and L. Z. Fan, *Energy Storage Mater.*, 2018, **15**, 37–45.
3 F. Bella, A. Verna and C. Gerbaldi, *Mater. Sci. Semicond. Process.*, 2018, **73**, 92–98.
4 M. Imperiyka, A. Ahmad, S. A. Hanifah and F. Bella, *Phys. B Condens. Matter*, 2014, **450**, 151–154.
5 F. Colò, F. Bella, J. R. Nair and C. Gerbaldi, *J. Power Sources*, 2017, **365**, 293–302.
6 R. Shanti, F. Bella, Y. S. Salim, S. Y. Chee, S. Ramesh and K. Ramesh, *Mater. Des.*, 2016, **108**, 560–569.
7 J. Cheng, G. He and F. Zhang, *Int. J. Hydrogen Energy*, 2015, **40**, 7348–7360.
8 K. Matsuoka, Y. Iriyama, T. Abe, M. Matsuoka and Z. Ogumi, *J. Power Sources*, 2005, **150**, 27–31.
9 D. García-Nieto and V. M. Barragán, *Electrochim. Acta*, 2015, **154**, 166–176.
10 R. Lan and S. Tao, *Electrochem. Solid-State Lett.*, 2010, **13**, B83.
11 E. Antolini and E. R. Gonzalez, *J. Power Sources*, 2010, **195**, 3431–3450.
12 H. Jung, H. Ohashi, T. Tamaki and T. Yamaguchi, *Chem. Lett.*, 2013, **42**, 14–16.
13 K.-D. Kreuer, *Chem. Mater.*, 2014, **26**, 361–380.
14 S. Miyanishi and T. Yamaguchi, *Phys. Chem. Chem. Phys.*, 2016, **18**, 12009–12023.
15 S. Miyanishi and T. Yamaguchi, *New J. Chem.*, 2017, **41**, 8036–8044.
16 Y. K. Choe, C. Fujimoto, K. S. Lee, L. T. Dalton, K. Ayers, N. J. Henson and Y. S. Kim, *Chem. Mater.*, 2014, **26**, 5675–5682.
17 K. Matsuyama, H. Ohashi, S. Miyanishi, H. Ushiyama and T. Yamaguchi, *RSC Adv.*, 2016, **6**, 36269–36272.
18 Z. Hu and S. Chen, in *Electrochemical Polymer Electrolyte Membranes*, 2015, pp. 495–537.
19 P. Hodge, G. a. Power and M. a. Rabjohns, *Chem. Commun.*, 1997, 73–74.
20 M. R. Hibbs, C. H. Fujimoto and C. J. Cornelius, *Macromolecules*, 2009, **42**, 8316–8321.
21 W.-H. Lee, E. J. Park, J. Han, D. W. Shin, Y. S. Kim and C. Bae, *ACS Macro Lett.*, 2017, **6**, 566–570.
22 J. S. Olsson, T. H. Pham and P. Jannasch, *Adv. Funct. Mater.*, 2018, **28**, 1–10.
23 H. Ono, T. Kimura, A. Takano, K. Asazawa, J. Miyake, J. Inukai and K. Miyatake, *J. Mater. Chem. A*, 2017, **5**, 24804–24812.
24 K. P. Weidkamp, A. Afzali, R. M. Tromp and R. J. Hamers, *J. Am. Chem. Soc.*, 2004, **126**, 12740–1.
25 S. Ando, A. Facchetti and T. J. Marks, *Org. Lett.*, 2010, **12**, 4852–5.
26 T. Uemura, M. Mamada, D. Kumaki and S. Tokito, *ACS Macro Lett.*, 2013, **2**, 830–833.
27 N. Misra and B. M. Mandal, *Die Makromol. Chemie, Rapid Commun.*, 1984, **5**, 471–475.
28 H. Peng, X. Sun, W. Weng and X. Fang, *Polymer Materials for Energy and Electronic Applications*, 2017.
29 L. Zhu, X. Yu and M. A. Hickner, *J. Power Sources*, 2018, **375**, 433–441.
30 J. Yan and M. A. Hickner, *Macromolecules*, 2010, **43**, 2349–2356.
31 L. Zhu, J. Pan, C. M. Christensen, B. Lin and M. A. Hickner, *Macromolecules*, 2016, **49**, 3300–3309.
32 G. S. Sailaja, S. Miyanishi and T. Yamaguchi, *Polym. Chem.*, 2015, **6**, 7964–7973.
33 J. Yan, L. Zhu, B. L. Chaloux and M. A. Hickner, *Polym. Chem.*, 2017, **8**, 2442–2449.
34 D. J. Kim, C. H. Park and S. Y. Nam, *Int. J. Hydrogen Energy*, 2016, **41**, 7649–7658.